Nuclear Materials Authority
P.O.Box 530 Maadi, Cairo, Egypt

DOAJ DIRECTORY OF OPEN ACCESS JOURNALS

ISSN 2314-5609
Nuclear Sciences Scientific Journal
9, 141- 151
2020
http://www.ssnma.com

URANIFEROUS DEPOSITS PROFILE IDENTIFICATION APPLYING NUCLEAR TRACKING TUBES TECHNIQUE

SAYED F. HASSAN; GEHAD M. SALEH; HAMED I. MIRA; AYMAN A. EL ABNOUDY and KORANY A. KORANY

Nuclear Materials Authority, Cairo, Egypt

ABSTRACT

Nuclear Tracking Tubes technique (NTT) is used to get the radon gradient as a function of depth. Accordingly, the shape and volume of uraniferous-ore body can be hypothetically determined. Using a grid net of Nuclear Tracking Tubes, depth and thickness of the uraniferous-ore body are profiled in Wadi Abu-Ruseid area, Southeast Egypt. The area of study is divided to Northern area (15 station) and Southern area (12 station). The data was found that radon diffusion is changed exponentially with the height of track detector from the earth crust. The volume of the southern part is nearly about twice of that of the northern part. The data through 3D visualization was cleared a global information about the ore body. The estimated volume of the northern area which containing the ore-body was found 1,449,500 m^3 with a roughly depth 70 m, while the data of the southern area is found about 2,347,200 m^3 at average depth 81m.

INTRODUCTION

^{222}Rn is a natural radioactive gas formed by ^{226}Ra radium decays in Earth crust. It is a noble gas with a half-life of 3.82 days, and may be released from ground and rocks. Diffusion and dispersion were partly responsible for radon transportation (Skeppstrom, and Olofsson, 2007). Radon escape to air through many factors as porosity, permeability and geological of rocks and soils (Somogyi, et al, 1986). Variation of radon concentration with depth has been discussed in several researches concerning transport pathway of radon gas from the deep layers (Abumurad, et al,1997a; Abumurad, et al,1997b; Al_shereideh, et al, 2006; Korany, et al, 2013). The dissection of exploratory drilling in uranium deposits, especially in the hard igneous rock sites, is difficult and more expensive to be carried out. The track detector method has been investigated to help in this study. The present study was investigated to assess the relation between radon activity concentration and both of thickness and depth at Abu-Rushied Area Southeast Egypt.

Next section is looking over the applied technique, the materials, and the methodology. Section three is discussing the results. Section four is covering the ore profile by a 3D visualization software. The conclusions are found in section five.

MATERIALS AND METHODOLOGY

Nuclear Track Tubes Technique

Track detectors (CR-39) were distributed inside hollow plastic tube as on Figs.1&2,

Plastic tube has radius 7 cm and length 60 cm. The number of track detectors inside the tube was ten. CR-39 sheet was cut it into 1cm x1cm. The tube is fitted vertically on the earth surface by using cement past.

CR-39 detectors were mounted inside the chamber tube at different heights by 5 cm apart between each other such as (12, 17, 22, 25, 27, 32, 37, 42, 47, 52 and 57 cm), (Fig.1 &2).

The radon-222 created due to natural radioactivity of radium-226 decay after its emanation in soils and rocks which passes through rock fractures and enters the plastic tube plastic tube as collimator. In this work, 270 detectors of CR-39 detectors (TD) were used. In the north and the south areas 15 and 12 tubes were placed respectively.

Fig. 1: Construction of Nuclear Track Tubes

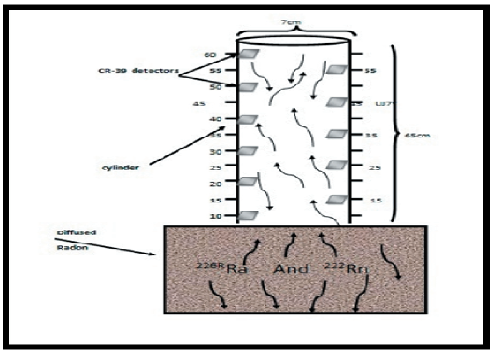

Fig. 2: Nuclear Track Tubes in the field

After exposure for certain time period, the tubes collected, detectors were taken, etched chemically and counted by using an optical microscope of magnification 640X for the tracks density calculation to estimate the radon gas concentration by employing the calibration factor for the used detectors (Hassan, 2015).

Rn gas gradient using SSNTDs employing Setup of Track Detectors

Poly-Allyi diglycol carbonate (CR-39) was used in this study, with a thickness of 500 µm, chemical formula $C_{12}H_{18}O_7$ and density 1.32 g.cm^{-3}. After exposure 10 days, the detectors were collected, chemically etched under optimum conditions using NaOH 6.25 N at 70 °C for 8 hours, radon gas concentration was calculated from the formula (Said, et al, 2009).

Then the radon gas concentration C_{Rn} can be estimated as

$$C_{Rn} = \rho / (T.K) \tag{1}$$

Where (ρ) is the corrected track density (number of tracks per cm^2/day), (K) is the obtained calibration factor (in this research is 0.221± 0.035 Track cm^{-2}day^{-1}/Bqm^{-3}), and T is the exposure time (day) (Said, et al, 2009).

Depth determination of subsurface radioactive anomalies

In this procedure, the diffusion process of radon has been determined by radon concentration gradient across (NTT). The measurements were done during summer season of each selected station. Radon inflow that occurred from deeply buried deposits is then migrating through cylindrical chamber which the detectors mounted at different heights. **Radon** transported to the surface detector mainly by diffusion and dispersion process from the point of origin through alpha-decay of ^{226}Ra atoms from the underground rock surface.

The relation between Diffusion Coefficient and Diffusion length of radon gas in the two media (air inside the tube and rock media) can be described by the following equation (Aly, et al, 2012).

$$D_{Rock} . X_{Rock} = D_{Air} . X_{Air} \quad (2)$$

Where D_{Rock} is diffusion coefficient of rock, D_{Air} is diffusion coefficient of air, X_{Rock} is diffusion length of rock and X_{Rock} is diffusion length of air.

Thickness determination of the radioactive layers under study

In this work, depth and thickness of the radioactive layer can be estimated by the following:

Case 1 *(Distance determination from the surface to the end of the radioactive source in the natural rock):*

For each station of the NTT grid we make fitting to the experimental data between the radon gas concentration (kBq/cm^3) and distance of each detector from the contact layers (cm) in the same station. It is observe that Rn-222 activity concentration is slightly decreased exponentially and then followed by randomly variations describing the successions of the overburden to the mineralized layers. The obtained curves can be fitted by a second degree relation as the following:

$$C_{Rn} = a(X_1)^2 + bX_1 \pm .c \quad (3)$$

Then the above equation is differentiate to get the maximum concentration gradient, we get

$$dC / dX = 2aX_1 + b \quad (4)$$

Equalizing the differentiated relation by zero, the inversion point of the curve (maximum value) could be detected, as $dC_{Rn} / dX = 0$ and hence the value of X_1 (X_{1Air}) was then calculated as:

$$0 = 2aX_1 + b \quad (5)$$

Then the radon diffusion coefficient in air is constant (D_{air}=1.2x10^5 m^{2}s^{-1}) and the values of the diffusion coefficient of the rock type under investigation D_{rock} could be obtained according to the geological rock formation (Aly, et al, 2012), which in is generally in the ranges of (10^{-8}-10^{-5}m^{2}s^{-1}) (Shweikani, et al, 1995). Then using equation (2), $X_{1(Rock)}$, which is the depth of the lower surface of the radioactive layer source, can be calculated (m) as follows:

$$X_{1(Rock)} = (D_{Air} . X_{1Air}) / D_{Rock} \quad (6)$$

Case 2 *(Distance determination from the surface to the Start of the radioactive source in the natural rock):*

Applying case 2 is carried out by cutting the upper obtained curve at the first most lower point before flocculation and then further getting the best fitting for the obtained relation, as:

$$C_{Rn} = a(X_2)^2 + bX_2 + c \quad (7)$$

Then again: $dC / dX = 2aX_2 + b$ (8)

Where C_{Rn} is the radon concentration; X_2 is the depth of the rock, that at depth (x) = 0, the flux density (J) = *b,* the radon concentration C at this theoretical initial moment has a very small value with theoretical zero distance upward to the earth surface, from the above equation, when $dC_{Rn}/dx=0$

$$0 = 2aX_2 + b \quad (9)$$

Then $X_{2(air)}$ (the distance of radon in air) can be determined, the diffusion of radon concentration decreases exponentially with the increase of soil thickness**.** Then applying Equation (2) again, we have:

$$D_{Rock} . X_{2Rock} = D_{Air.} X_{2Air}$$

Where, X_{2Rock} is the depth of the upper surface of the radioactive layer source, which can be calculated (in terms of meter) as follows:

$$X_{2(Rock)} = (D_{Air} . \quad) / D_{Rock} \quad (10)$$

Finally we could get the radioactive layer thickness as:

$$Layer\ Thickness = X_{1(Rock)} - X_{2\ (Rock)} \qquad (11)$$

Which has a depth of $X_{2(Rock)}$ from the surface for each station of the NTT grid net.

RESULTS AND DISCUSSIONS FOR A CASE STUDY

Geology of the Area Under Study

A study was undertaken for the assessment of radioactive anomaly thickness at Abu-Rushied Area Southeast Egypt.

The study area lies in the southern part of the Eastern Desert of Egypt at the boundary between Central Eastern Desert (CED) and the Southern Eastern Desert (SED) at about 90 km southwest of Mersa Alam. It is limited by latitudes 24° 37' 25" and 24° 38' 17" N and longitude 34° 45' 30" & 34° 46' 29" E. The study area divided into two sections: Northern area and southern area separated by barren area, (Fig. 3).

The present work aims to evaluate the depth and thickness of the uraniferous-ore body then the total ore volume in the area under investigation using Tracking Tubes technique (NTT), in which CR-39 detectors are used in measuring the radon gas concentration at various tube heights. The Experimental data was used to fit the depth profile function of radon level measurements.

Depth and Thickness Evaluation

The radon concentration measurements (Bqm^{-3}) are applied in calculating the depth and thickness of the rock radioactivity and the height of each detector set from the bottom of the tube for each station.

The Northern area

For the first station, all the data of the ten detectors are taken into consideration to determine the thickness and depth of the radioactive layer as shown on Fig. (4).

Figure (4) represents the relationship between radon concentration (kBq/cm^3) and

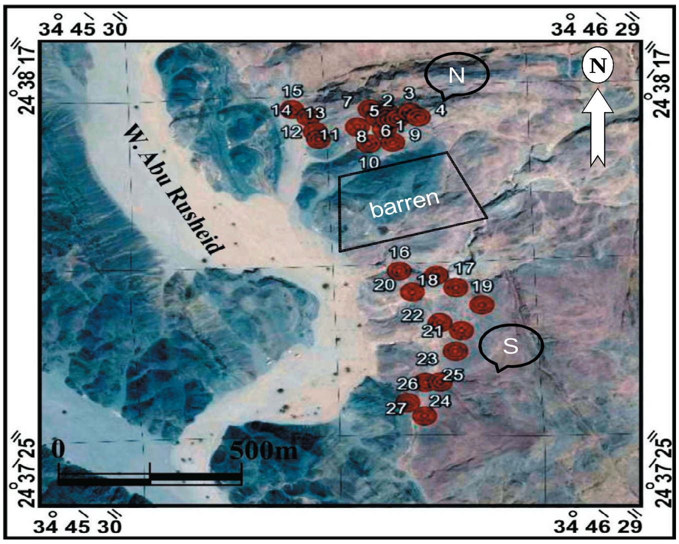

Fig. 3: Land sat image of the stations selected of Wadi Abu-Rushied

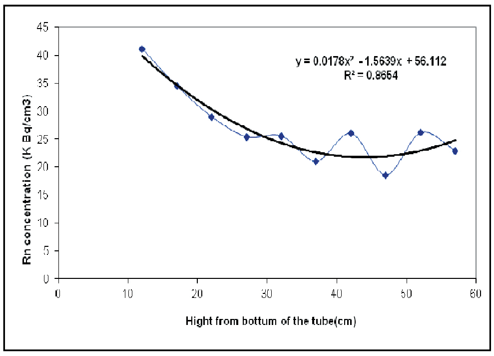

Fig. 4: Radon gas gradient for station 1, case one

CR-39 detector height (cm) for the estimation of the depth (m) for the lower surface of the rock layer. The fitting of the experimental data is shown in the relation:

$C_{Rn} = 0.017(X_1)^2 - 1.563X_1 + 56.1$

Where C_{Rn} is the radon concentration and X is the depth for the rock. The radon concentration C at this theoretical initial moment has a very small value with theoretical zero distance upward to the earth surface, from the above equation, when:

$(dC / dX) = 0$ Then

$dC / dX = 0.034X_1 - 1.563 = 0$

$X_1 = 45.97$ Cm

Where X_1: is the diffusion distance of radon in air.

Our data of diffused radon in air is found consistent with the literature (Shweikani, et al, 1995) by using the relation between diffusion length and diffusion coefficient of radon eq. (2).

$X_{1(Rock)} = (D_{Air} . \quad) / D_{Rock}$

Where: X_{1Rock} is the depth of the lower surface of the radioactive layer at this NTT net point. By substituting in the above eq., we found.

$X_{1(Rock)} = [1.2 \times 10^{-5} (m) \times 45.97 \times 10^{-2} (m)] / [0.053 \times 10^{-6} (m)]$

$X_{1Rock} = 104.1m$

For the second case, taking the points which give homogenous curve of second order is done to determine the depth of the deposit layer.

Figure (5) represents the relation between radon concentration and CR-39 detector height (cm) for the estimation of the depth (m) for the upper rock radioactive layer.

$C_{Rn} = 0.044(X_2)^2 - 2.766X_2 + 68.15$

Where: C_{Rn} is the radon concentration and X is the depth for the rock. The radon concentration variations stop at path length of radon movement into air, from the above equation, when:

$(dC / dX) = 0$ Then

$(dC / dX) = 0.088X_2 - 2.766 = 0$

$X_2 = 31.43$ Cm

Where: X_2 is the diffusion distance of radon in air, and as explained before, we get

$X_{2(Rock)} = (D_{Air} . \quad) / D_{Rock}$

Where, X_{2Rock} is the depth of the upper surface of the radioactive layer at this NTT net point.

$X_{2(Rock)} = [1.2 \times 10^{-5} (m) \times 31.43 \times 10^{-2} (m)] / [0.053 \times 10^{-6} (m)]$ Thus:

$X_{2Rock} = 71.2m$

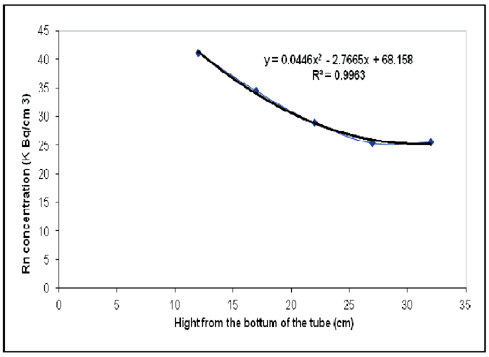

Fig. 5: Radon gas gradient for station 1, case two

Then the value of the bearing-uranium layer thickness at this NTT net point is:

Layer Thickness = $X_{1(Rock)} - X_{2\ (Rock)}$

Layer Thickness = 104.1 - 71.2

Layer Thickness = 32.9 m

Accordingly, at a depth of 71.2 m from the surface at this station the ore thickness is 32.9 m.

Following the same manner for the case one and case two estimations for each NTT station, to get X_{1Rock}, X_{2Rock} and the layer depth and thickness, a dissection with good information about the core of the ore rocks in Northern area could be detailed.

Data for all stations of the northern part were summarized in (Table 1), including radon gradient for case one and case two, X_{1Rock}, X_{2Rock}, and thickness.

The Southern area

Both cases were also applied for each station in the Southern part to get X_{1Rock}, X_{2Rock} and finally the layer thickness in meter. The data of both cases for all stations in the southern part were summarized in (Table 2).

Three-Dimensional (3-D) Visualization of the Ore-Body

General description of the ore-body

The ore-body in the studied area is consisting mainly from two parts: the northern and the southern parts. The description of the above two parts was explained on the NTT data for both of the depth and thickness by their integrations. In addition, these descriptions are perceived and realized through a three-dimensional (3-D) visualization of the two ore-body parts. The 3D-visualization of the ore-body parts is made by the assistance of the program package MINESIGHT® that developed by MINTEC, Inc. (Tucson, Arizona). The methodology employed for this software is to consider the NTT data as two-

Table 1 : Uraniferous layer depth and thickness (Northern area)

S. No.	R_n gradient / Case one	X_{1Rock} (m)	R_n gradient / Case two	X_{2Rock} Depth (m)	Thickness (m)
1	$C = 0.017X_1^2 - 1.56X_1 + 56.11$	104.1	$C = 0.044X_2^2 - 2.76X_2 + 68.15$	**71.2**	**32.9**
2	$C = 0.003X_1^2 - 0.287X_1 + 37.75$	108.3	$C = 0.013X_2^2 - 0.939X_2 + 46.08$	**81.7**	**26.5**
3	$C = 0.047X_1^2 - 2.51X_1 + 164.6$	60.5	$C = 0.219X_2^2 - 11.17X_2 + 258.8$	**43.5**	**16.9**
4	$C = 0.031X_1^2 - 1.65X_1 + 21.14$	60.4	$C = 0.119X_2^2 - 5.4X_2 + 93.33$	**51.4**	**9.0**
5	$C = 0.005X_1^2 - 0.423X_1 + 17.41$	96.0	$C = 0.011X_2^2 - 0.747X_2 + 21.14$	**76.8**	**18.9**
6	$C = 0.034X_1^2 - 2.954X_1 + 134.7$	98.4	$C = 0.051X_2^2 - 4.039X_2 + 148$	**89.7**	**8.6**
7	$C = 0.067X_1^2 - 6.938X_1 + 359.6$	117.1	$C = 0.119X_2^2 - 10.01X_2 + 396.7$	**95.2**	**21.8**
8	$C = 0.101X_1^2 - 5.96X_1 + 109$	66.8	$C = 0.106X_2^2 - 5.93X_2 + 106.7$	**63.3**	**3.5**
9	$C = 0.008X_1^2 - 0.788X_1 + 98.59$	111.5	$C = 0.137X_2^2 - 6.966X_2 + 162.8$	**57.6**	**53.9**
10	$C = 0.022X_1^2 - 1.689X_1 + 74.38$	86.9	$C = 0.031X_2^2 - 2.219X_2 + 80.8$	**81.0**	**5.9**
11	$C = 0.015X_1^2 - 1.35X_1 + 43.26$	101.9	$C = 0.033X_2^2 - 1.918X_2 + 47.39$	**65.8**	**36.1**
12	$C = 0.009X_1^2 - 0.78X_1 + 25.83$	98.1	$C = 0.019X_2^2 - 1.345X_2 + 32.18$	**80.1**	**18.0**
13	$C = 0.062X_1^2 - 5.55X_1 + 217.1$	101.3	$C = 0.061X_2^2 - 52.67X_2 + 211.3$	**97.7**	**3.5**
14	$C = 0.027X_1^2 - 2.263X_1 + 121.2$	94.9	$C = 0.127X_2^2 - 7.186X_2 + 174$	**64.1**	**30.8**
15	$C = 0.046X_1^2 - 4.691X_1 + 168$	115.4	$C = 0.059X_2^2 - 5.551X_2 + 179.2$	**106.5**	**8.9**

Table 2: Uraniferous layer depth and thickness (Southern area)

S. No.	R_n gradient / Case one	X_{1Rock} (m)	R_n gradient / Case two	X_{2Rock} Depth (m)	Thickness (m)
16	$C = 0.035X_1^2 - 2.365X_1 + 212$	76.5	$C = 0.207X_2^2 - 10.59X_2 + 298.4$	57.9	18.5
17	$C = 0.005X_1^2 - 0.569X_1 + 26.72$	128.8	$C = 0.01X_2^2 - 0.85X_2 + 30.26$	95.7	33.1
18	$C = 0.010X_1^2 - 1.013X_1 + 36.41$	114.7	$C = 0.018X_2^2 - 1.385X_2 + 40.29$	87.1	27.6
19	$C = 0.012X_1^2 - 1.103X_1 + 58.87$	104.1	$C = 0.015X_2^2 - 1.314X_2 + 61.56$	99.2	4.9
20	$C = 0.006X_1^2 - 0.612X_1 + 21.83$	115.5	$C = 0.016X_2^2 - 1.126X_2 + 27.48$	79.7	35.8
21	$C = 0.002X_1^2 - 0.203X_1 + 15.44$	114.9	$C = 0.004X_2^2 - 0.352X_2 + 17.28$	99.6	15.3
22	$C = 0.004X_1^2 - 0.448X_1 + 20.14$	126.8	$C = 0.009X_2^2 - 0.661X_2 + 22.36$	83.1	43.6
23	$C = 0.019X_1^2 - 1.456X_1 + 60.50$	86.8	$C = 0.033X_2^2 - 2.286X_2 + 70.59$	78.4	8.3
24	$C = 0.018X_1^2 - 1.615X_1 + 104.2$	101.6	$C = 0.061X_2^2 - 3.66X_2 + 125.3$	67.9	33.64
25	$C = 0.002X_1^2 - 0.230X_1 + 8.52$	130.2	$C = 0.005X_2^2 - 0.368X_2 + 10.08$	83.3	46.9
26	$C = 0.009X_1^2 - 0.944X_1 + 51.76$	118.7	$C = 0.016X_2^2 - 1.313X_2 + 55.69$	92.9	25.8
27	$C = 0.011X_1^2 - 1.033X_1 + 55.83$	106.3	$C = 0.03X_2^2 - 1.97X_2 + 65.74$	74.4	31.9

intervals boreholes of binary (0,1): the (zero) interval symbolizes the upper surface depth of the ore-body while the (one) symbolizes its thickness.

Northern Part

The Ore-body in northern part (trend and volume)

In general, the northern part takes a main trend of a deviation 250° for its inclination with a dip angle of about 30° SW, (Fig. 6). The approximate estimated volume of the northern part of the ore-body is about 1,449,500 m^3.

Depth readings interpretation (Northern part)

The depth of the northern part is in general compatible with its inclination to the west. The average of the arithmetic and engineering means of the depth is about 70m. The maximum depth for this part is mainly located at its northern-west region, which is reaching to about 107m.

The depth is slightly decreasing to the east until reaching its minimum at the south-eastern region, which is about 44m. The depth is also gradually decreasing to the northern east and reaching to about 52m, (Fig. 7).

Thickness data interpretation (Northern part)

The thickness of the ore-body northern part is in general non-uniform. This gives the ore-body a rather complicated shape as viewed on Fig.(7). The average of the arithmetic and engineering means of the thickness is about 20m, which is prevailing at the western-middle region of the ore-body, (Fig. 8). The center of the south-western region of the ore-body records the maximum thickness, which is about 54m. In the middle of the most northern region, there is also a rather thick part of about 31m.

This region is then gradually decreased from the western towards the eastern directions until reached to min. 4m and 15m, respectively. Also, the highest two regions were decreased until reached to about 9m at the most northern east.

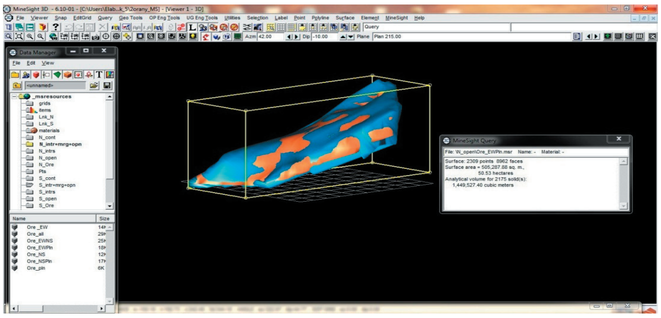

Fig. 6: The ore-body Northern part contained in the measuring volume cuboid at an azimuth 42 °

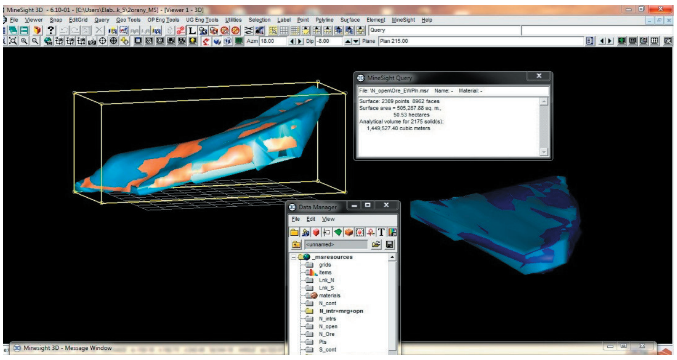

Fig. 7: Screenshot for both Northern & Southern parts of the ore-body at an azimuth 18 °

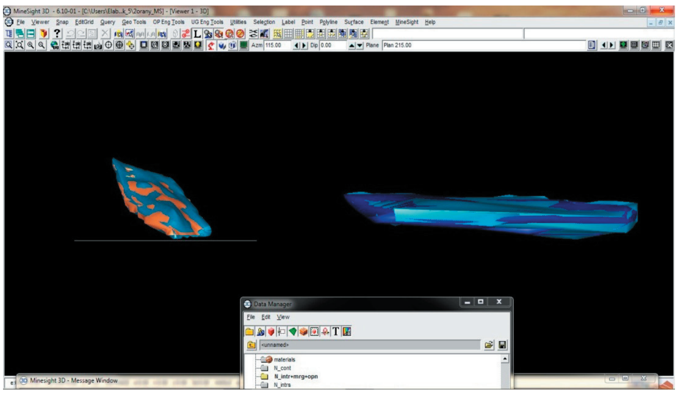

Fig. 8: Screenshot for both Northern & Southern parts of the ore-body at an azimuth 115°

Southern Part

The Ore-body in Southern part (trend and volume)

In general, the southern part has obviously a more gently dipping angle than the northern one, while its volume is larger by about 62%. The southern part takes the trend of a deviation 195° for its inclination with a dip angle of about 15° S. The approximate estimated volume of the southern part of the ore-body is about 2,347,200 m^3, (Fig. 9).

Depth data interpretation (Southern part)

The depth of the southern part has an average of the arithmetic and engineering means of about 81m. The maximum depth for this part is located at its northern-east region of the ore-body, which is reaching to about 100m. The depth is then slightly decreasing in two directions. It decreases gradually by going to the west direction until reaching to about 67m at the northern west region.

In the same time, the depth is also decreasing as going south until reaching to the minimum depth of about 58m at the most southern region, (Fig. 10).

Thickness readings interpretation (Southern part)

The thickness of the ore-body southern part is in general more stable and uniform than that belonging to the northern ore-body part. The average of the arithmetic and engineering means of the thickness of this part is about 28m. This mean thickness is almost prevailing throughout the whole ore-body area except for the most northern region.

At the most northern region, the thickness is decreasing until reaching its minimum record, which is about 8m, at the north eastern region. The maximum thickness is recorded at south eastern region of the ore-body, which is about 36m.

CONCLUSION

In this research, track detectors method inside tubes, which is called "Tracking Tubes technique (NTT)", was used to measure radon activity concentration emitted from earth crust. The depth and thickness of the uraniferous-ore body were hypothetically determined in Wadi Abu-Ruseid area, Southeast Egypt. This method was used to get the radon gradient through depth and consequently de-

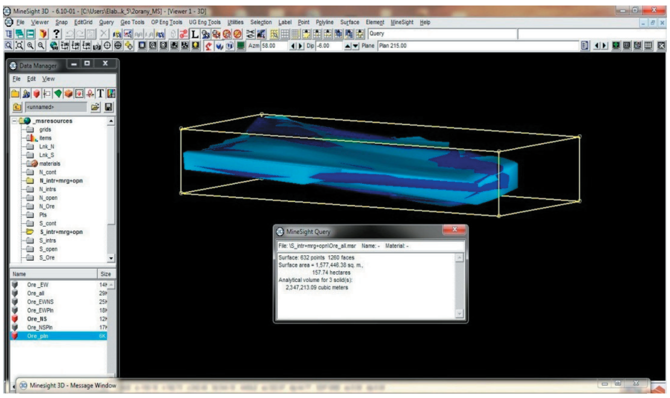

Fig. 9: The ore-body Southern part contained in the measuring volume cuboid at an azimuth 58°

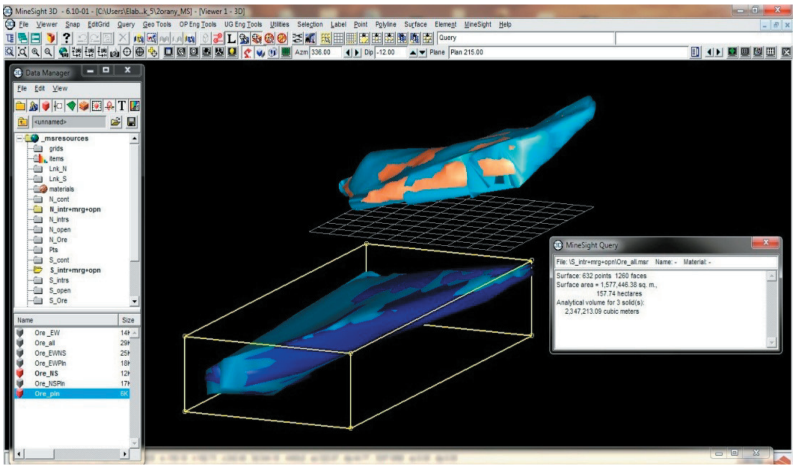

Fig. 10: Screenshot for both Northern & Southern parts of the ore-body at an azimuth 336°

termination the volume and shape of uraniferous-ore body at the two parts. The radon gas concentrations gradient was found to have exponentially behavior for all station. The software MINESIGHT is used to set 3-D visualization of the two parts area (North and South) which gives good information about the ore body. The total volume of the northern part was 1,449,500 m3, while the total volume of the southern part is about 2,347,200 m3, which is about 62% larger than the volume of the southern part.

REFERENCES

Abumurad, K.M.; Al-Bataina, B.; Ismail, A. and Kullab, M., 1997a. A survey of radon levels in Jordanian dwellings during an autumn season. Rad. Prot. Dos., 69, 221-226.

Abumurad, K.M.; Atallah, M.; Kullab, M.K. and Ismail, A.A., 1997b. Survey of radon levels in Jordanian dwellings during an autumn season. Rad. Measurement, 28, 585-588.

Al_shereideh, S.A.; Bataina, B.A. and Ershaidatb, N.M., 2006. Seasonal variations and depth dependence of soil radon concentration levels in different geological formations in DeirAbu-Said District, Irbid. Jordan. Rad. Measurements, 41, 703-707.

Aly, H.A.; Hegazy, T.M.; Abdel_Ghany, H.A.; Abu_Zied, H.M.; El-Aassy, I.E. and Shaaban, D.H., 2012. Determination of subsurface radioactive anomalies using alpha particle measurements of diffused radon. Iso. Rad. Res, 44, 89-101.

Hassan, S.F, 2015. Depth determination of the subsurface uranium deposits using CR-39 cylindrical technique in Gneissoic granitic rocks, Abu Rushied area, Southeastern Desert, Egypt. J. Rad. Research and App. Science, 8, 562-569.

Korany, K.A.; Shata, A.E.; Hassan, S.F. and El Nagdy, M.S., 2013. Depth and seasonal variation for the soil radon-gas concentration level at wadi Nasieib area, southwestern, Egypt. J. phys. Chem. and Biophysics, 4, 123-133.

Said, A.F.; Hassan, S.F.; Orabi, F.M. and Abdel-Razek, Y.A., 2009. Uranium Prospecting using CR-39 Etch Track Detector at Abu Rusheid Area, South Eastern Desert, Egypt. Internal report, Nuclear Materials Authority, Egypt.

Shweikani, R.; Giaddui, T.G. and Durrani, S.A., 1995. The effect of soil parameters on the radon concentration values in the environment. Rad. Measurements, 25, 581-584.

Skeppstrom, K. and Olofsson, B., 2007. Uranium and radon in groundwater, an over view of problem. European Water ,17/18, 51- 62.

Somogyi, G.; Hafez, A.; Hunyadi, I. and Szilagyi, M., 1986. Measurement of exhalation and diffusion parameters of radon in solids by plastic track detectors. Nuclear Radiation Measurement, 12, 701-704.

التعرف علي حدود الترسبات الاشعاعية بتطبيق تقنية انابيب التتبع النووي

سيد فهمي حسن ، جهاد محمد صالح ، حامد ابرهيم ميرة ، أيمن عبد الفتاح الأبنودي و قرني أحمد قرني

تستخدم تقنية انابيب التتبع النووي في الحصول علي معدل تغير غاز الرادون مع العمق و بالتالي نتمكن من تعيين الشكل و الحجم الافتراضيين للترسيبات الاشعاعية . بأستخدام شبكة من انابيب التتبع النووي , امكن عمل شكل تصوري لعمق و سمك الجسم الحاوي للخام المشع بمنطقة ابو رشيد - جنوب شرق مصر. و قد تم تقسيم منطقة الدراسة الي جزيئين رئيسيين: الشمالي (١٥ نقطة قياس) و الجنوبي (١٢ نقطة قياس) .

وقد اظهرت النتائج ان انبعاث الرادون يتغير بطريقه أسيه مع ارتفاع كاشف الاثر النووي عن قاع الانبوبة . و قد وجد ان حجم الجزء الجنوبي يقدر تقريبا بضعف الجزء الشمالي كما أظهر التمثيل ثلاثي الابعاد بعض المعلومات الهامة حول الجسم الحاوي للخام حيث وجد ان الحجم التقديري المحسوب للجزء الشمالي للجسم الحاوي للخام يقدر بحوالي ١,٤٤٩,٥٠٠ متر مكعب بينما متوسط العمق التقديري كان حوالي ٧٠ متر , بينما كان الحجم التقديري المحسوب للجزء الجنوبي حوالي ٢,٣٤٧,٢٠٠ متر مكعب بمتوسط عمق حوالي ٨١ متر.